

Analysis Quality Factor in Two-Dimensional Photonic Crystal by the FDTD Method

Sh. Ghorbnzadeh

Department of Engineering, Aliabad Katoul Branch, Islamic Azad University, Aliabad Katoul, Iran

Abstract: One of the present challenges in challenges in telecommunication technology is implementation of photonic integrated circuits (PICs), with ability to perform efficiently different tasks. Increasing in volume of information and instruments, makes this technology going to the way of integration and it needs a material to be the base of this revolution. One of the materials that can contain these characteristics with the dimensions near the visible light wavelength is photonic crystal, the best known material to reach the goal. Anisotropic materials that their refractive index is a periodic function of place with the periodicity near the wavelength of the visible light. They are known as crystals, because of making with repetition of one building block. Also, the word "photonic" is used, as they affect the properties of photons' propagation. If a single point defect is created in the structure some resonant modes appear in the band gap. We show that the properties of these modes can be controlled by simply changing the nature and size of the defects. We compute the frequency, polarization and field distribution of the resonant modes by solving Maxwell's equations in the frequency domain. The dynamic behavior of the modes is determined by using a finite-difference time-domain method which allows us to compute the coupling efficiency and the losses in the micro cavity.

Key words: Photonic crystal % Quality factor % FDTD

INTRODUCTION

Photonic crystals provide a possibility of eliminating electromagnetic wave propagation within a frequency band, i.e., a photonic band gap (PBG). [1] If a defect is Introduced in an otherwise perfect photonic crystal, a mode (or group of modes) may be found at a frequency (or some frequencies) within the PBG [2-3] It is crucial to understand the nature of such localized modes for potential applications of doped photonic crystals in lasers, resonators and wavelength division multiplexing (WDM). [4] Theoretical studies of defect modes employ a wide variety of numerical techniques, including plane-wave expansion method, exact Green's function method, transfer matrix method and a finite-difference time-domain (FDTD) method with a dipole source located near the defect. All these methods are based on a super cell technique, in which the defect is placed in each repeated super cell of a sufficiently large size.

If a small defect is introduced in the photonic crystal, a mode (or group of modes) can be created within the structure at a frequency which lies inside the gap.

The defect behaves like a micro cavity surrounded by reflecting walls. If the defect has the proper size to support a state in the band gap and if the radiative transition frequency of the atom matches that of the defect state, the rate of spontaneous emission will be enhanced method is applicable to any form of dielectric and/or metallic inclusions.

Numerical Model and Method: A defect can be introduced into a photonic crystal by removing one or several unit cells, or replacing them with other materials, or just changing the shape of inclusions, etc [4]. to investigate the properties of defect states in photonic crystals, two different computational approaches are used. The first solves Maxwell's equations in the frequency-domain, while the second solves the equations in the time-domain. These two methods reveal different information about the cavity. The frequency-domain method yields the frequency, polarization, symmetry and field distribution of every eigenmode in the cavity and the time-domain method allows us to determine the temporal behavior of the modes By looking at the evolution of the

fields in time, we will be able to determine the coupling efficiency, the scattering the quality factor of the cavity.

Frequency Domain: In the first method, the fields are expanded into a set of harmonic modes; the wave equation for the magnetic field is written in the form

$$\nabla \times \left\{ \frac{1}{\mathbf{e}(r)} \nabla \times \mathbf{H}(r) \right\} = \frac{\omega^2}{c^2} \mathbf{H}(r) \quad (1)$$

where $c = \frac{1}{\sqrt{\mu_0 \epsilon_0}}$ is the speed of the light.

Equation (1) is an eigenvalue problem which can be rewrite as

$$\mathbf{1} h_n = \mathcal{G}_n H_n \quad (2)$$

where $\mathbf{1}$ is a Hermitian differential operator and \mathcal{G}_n is the nth eigenvalue, proportional to the squared frequency of the mode.

We solve Eq.(2) by using a variational approach, where each eigenvalue is computed separately by minimizing the functional $\langle H_n | \Theta | H_n \rangle$.

Briefly, to find the minimum, we use the conjugate gradient method with preconditions, keeping H_n orthogonal to the lower states. The conjugate gradient method has the advantage of being more efficient than the traditional method of steepest descents, In order to minimize the functional, we need to calculate

$$\Theta H_n(r) = \left\{ \nabla \times \frac{1}{\mathbf{e}(r)} \nabla \times \right\} H_n(r) \quad (3)$$

Time Domain: The second method solves Maxwell's equations in real space, where the explicit time dependency of the equations is maintained equations can be written in the following form,

$$\frac{d\mathbf{H}}{dt} = -\frac{1}{\mathbf{m}} \nabla \times \mathbf{E} \quad (4)$$

$$\frac{\partial \mathbf{E}}{\partial t} = \frac{1}{\mathbf{e}(r)} \nabla \times \mathbf{H} - \frac{\partial(r)}{\mathbf{e}(r)} \mathbf{E} \quad (5)$$

where $\mathbf{g}(r)$, $\mu(r)$ and $\mathbf{F}(r)$ are the position dependent permittivity, permeability and conductivity of the material, respectively. In a two-dimensional case, the fields can be decoupled into two transversely polarized modes, namely, the E polarization and the H polarization. These equations can be discretized in space and time by a so-called

Yee-cell technique. The following FDTD time stepping formulas are the spatial and time discretizations of Eqs. (3) and (4) on a discrete two-dimensional mesh within the x- y coordinate system for the E polarization,

$$H_x \Big|_{i,j+\frac{1}{2}}^{n+\frac{1}{2}} = H_x \Big|_{i,j+\frac{1}{2}}^{n-\frac{1}{2}} - \frac{\Delta t}{\mathbf{m}_{x,j+\frac{1}{2}}} \frac{E_z \Big|_{i,j+1}^n - E_z \Big|_{i,j}^n}{\Delta y} \quad (6)$$

$$H_y \Big|_{i+\frac{1}{2},j}^{n+\frac{1}{2}} = H_y \Big|_{i+\frac{1}{2},j}^{n-\frac{1}{2}} + \frac{\Delta t}{\mathbf{m}_{y+\frac{1}{2},j}} \frac{E_z \Big|_{i+1,j}^n - E_z \Big|_{i,j}^n}{\Delta x} \quad (7)$$

$$H_z \Big|_{i,j}^{n+1} = \left(\frac{\mathbf{e}_{i,j} - \mathbf{S}_{i,j} \frac{\Delta t}{2}}{\mathbf{e}_{i,j} + \mathbf{S}_{i,j} \frac{\Delta t}{2}} \right) E_z \Big|_{i,j}^n + \frac{\Delta t}{\mathbf{e}_{i,j} + \mathbf{S}_{i,j} \frac{\Delta t}{2}} \left(\frac{H_y \Big|_{i+\frac{1}{2},j}^{n+\frac{1}{2}} - H_y \Big|_{i-\frac{1}{2},j}^{n+\frac{1}{2}}}{\Delta x} - \frac{H_x \Big|_{i,j+\frac{1}{2}}^{n+\frac{1}{2}} - H_x \Big|_{i,j-\frac{1}{2}}^{n+\frac{1}{2}}}{\Delta y} \right) \quad (8)$$

where the index n denotes the discrete time step, indices i and j denote the discretized grid point in the x-y plane, respectively.) t is the time increment and) x and) y are the intervals between two neighboring grid points along the x and y directions, respectively. Similar equations for the H polarization can be easily obtained.

Special consideration should be given at the boundary of the finite computational domain, where the fields are updated using special boundary conditions as information out of the domain is not available. Here, we use the perfectly matched layer (PML) method for the boundary treatment. In the PML, the electric or magnetic field components are split into two subcomponents i.e., $E_x = E_x + E_{x,y}$ in the E-polarization case (with the possibility of assigning losses to the individual split field components. The net effect of this is to create an absorbing medium which is nonphysical) adjacent to the outer FDTD mesh boundary such that the interface between the PML and the FDTD mesh is reflectionless for all frequencies, polarizations and angles of incidence. The FDTD technique can be applied directly for the numerical implementation of the fields inside the PML without any special treatment (the details can be found in, e.g., Ref. 6). If one knows all the necessary information at each space grid point, such as the permittivity, Permeability, conductivity and the initial distribution of the fields, one can obtain the time evolution of the fields by the discretized FDTD time-stepping formulas. Therefore, this method can be easily applied to any form of inclusions, dielectric and/or metallic. The FDTD time-stepping formulas are stable numerically if the following condition is satisfied,

$$\Delta t \leq \frac{1}{c\sqrt{\Delta x^{-2} + \Delta y^{-2}}} \quad (9)$$

where c is the speed of the light.

Two-Dimensional Crystals: We begin by investigating the properties of a micro cavity in a two-dimensional photonic crystal. The crystal consists of a perfect array of infinitely long dielectric rods located on a square lattice of length a . Each rod has a radius of $0.20a$ and a refractive index of 3.4 . By normalizing every parameter with respect to the lattice constant a , we can scale the micro cavity to any length scale simply by scaling a .

Mode Symmetry: We investigate the propagation of electromagnetic fields in the plane normal to the rods. Since the rods have translational symmetry along their axes, the waves can be decoupled into two transversely polarized modes, transverse electric (TE) and transverse magnetic (TM), depending on whether the electric or magnetic field is normal to the rods. that there is a large photonic band gap for the E polarization between the frequencies $0.29 (2Bc/a)$ and $0.42 (2Bc/a)$ Fig 1. A defect is now introduced into the perfect array of rods. The defect can have any shape or size; it can be made by changing the refractive index of a rod, modifying its radius, or removing a rod altogether. The defect could also be made by changing the index or the radius of several rods. Here we choose to modify the radius of a single rod. The modes in the crystal are computed using a supercell approximation, which consists of placing a large crystal with a defect into a super cell and repeating it periodically in space. In the example below, the supercell contains a 7×7 crystal [5].

A defect is now introduced into the perfect array of rods. The defect can have any shape or size; it can be made by changing the refractive index of a rod, modifying its radius, or removing a rod altogether. The defect could also be made by changing the index or the radius of several rods. Here we choose to modify the radius of a single rod. The modes in the crystal are computed using a supercell approximation, which consists of placing a large crystal with a defect into a super cell and repeating it periodically in space. In the example below, the supercell contains a 7×7 crystal. We begin with a perfect crystal—where every rod has a radius of $0.2a$ —and gradually reduce the radius of a single rod. Initially, the perturbation is too small to localize a mode in the crystal.

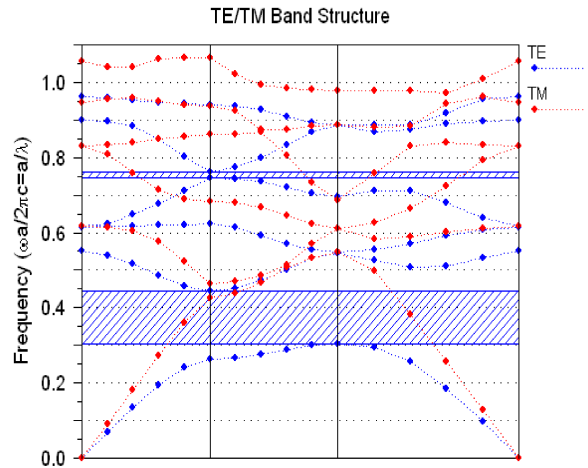


Fig. 1: Band diagram for E and H polarizations. Band gaps exist only in the case of E-polarization (gray areas)

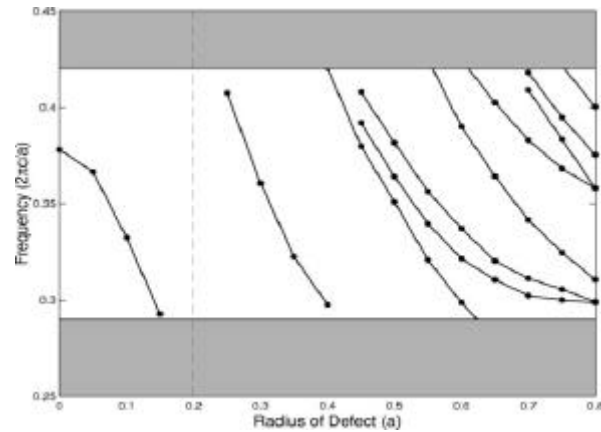


Fig. 2: Frequency of the defect states in an array of dielectric rods with radius $0.20a$. The defect is introduced by changing the radius R of a single rod. The case where $R = 0.20a$ corresponds to a perfect array, while the case where $R = 0$ corresponds to the removal of a rod. The shaded regions indicate the edges of the band gap.

When the radius reaches $0.15a$, a resonant mode appears in the vicinity of the defect. Since the defect involves removing dielectric material in the crystal, the mode appears at a frequency close to the lower edge of the band gap. As the radius of the rod is further reduced, the frequency of the resonant mode sweeps upward across the gap and eventually reaches $f = 0.38c/a$ when the rod is completely removed. Figure 2 shows the frequency of the mode for several values of the radius. The frequency of the mode can be tuned by simply adjusting the size of the rod. cell and repeating it periodically in space. In the example below, the supercell contains a 7×7 crystal.

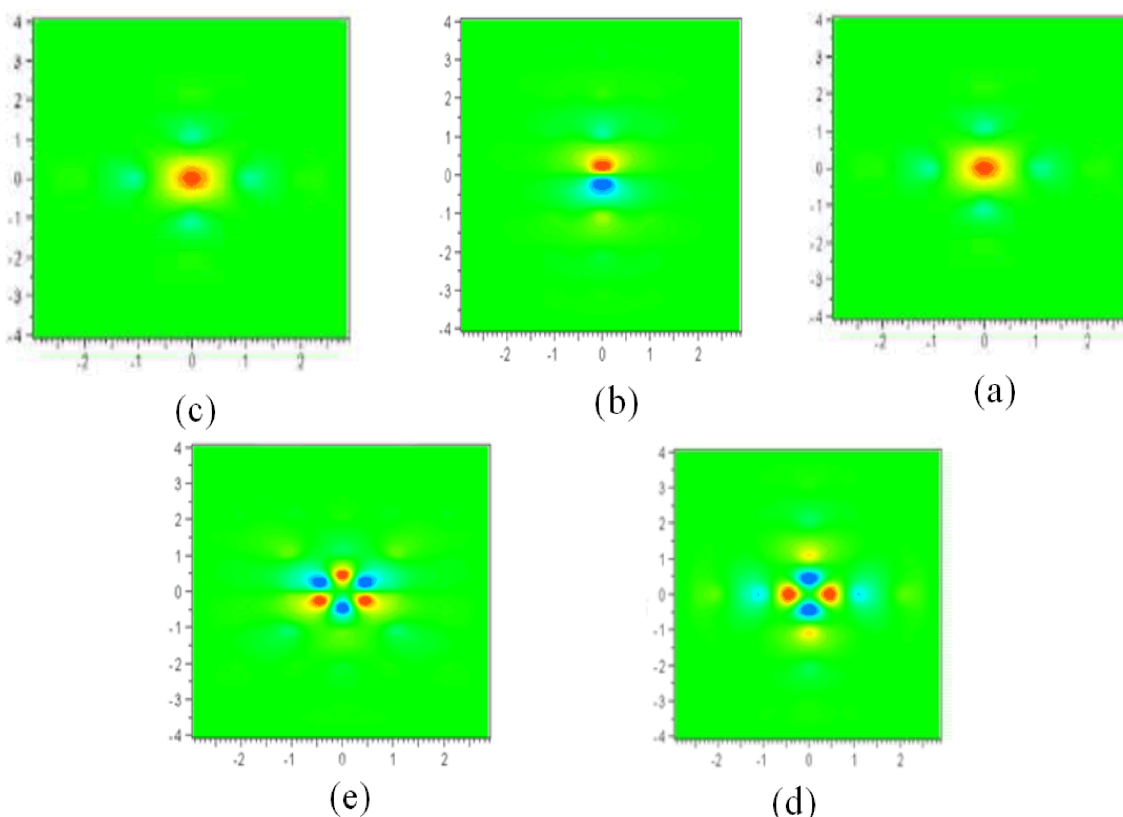


Fig. 3: Electric-field distribution of TE defect states in an array of dielectric rods for various defect sizes. (a) Monopole, $R=0.10a$ (b) Doubly degenerate dipoles, $R=0.33a$, $R=0.60a$. (c) Second-order monopole, $R=0.60a$. (d) and (e) Doubly degenerate hexapoles, $R=0.60a$. The white circles indicate the position of the rods.

The electric field distribution of the resonant mode is shown in Fig. 2(a) for the specific case where the radius is equal to $0.10a$. The electric field is polarized along the axis of the rods and decays rapidly away from the defect. Since the field does not have a node in the azimuthal direction, it is labeled a monopole. The frequency of the mode is $f = 0.32c/a$. Instead of reducing the size of a rod, it would also have been possible to increase its size. Again, starting from a perfect crystal, we gradually increase the radius of a rod. When the radius reaches $0.25a$, one doubly degenerate modes appear at the top of the gap. Since the defect involves adding material, the modes sweep downward across the gap as the radius increases. The modes eventually disappear into the continuum below the gap when the radius becomes larger than $0.40a$ (Fig. 2).

The field distribution of the one doubly degenerate mode is shown in Figs. 3(b) for the case where $R=0.33a$. The modes are labeled dipoles since they have two nodes in the plane. By increasing the radius further, a large number of resonant modes can be created in the vicinity

of the defect. This is shown again in Fig. 2. Several modes appear at the top of the gap: first a quadrupole, then another (nondegenerate) quadrupole, followed by a second-order monopole and two doubly degenerate hexapoles. These modes also sweep downward across the gap as the defect is increased. The modes are shown in Figs. 3(c)–3(d) and 3(e) for the case where $R = 0.60a$. The defect state resembles a whispering-gallery mode found in a microdisk laser. The field has many nodes (12 in this case) and is located mostly at the edges of the defect [8-9].

Quality Factor: The quality factor Q is a measure in the cavity. Since the reflectivity of the crystal surrounding the defect increases with the size of the crystal. To compute Q we choose to use an approach which first involves pumping energy in to the cavity then monitoring its decay. We recall the quality factor is defined as

$$Q = \frac{w_0}{P} = -\frac{w_0 E}{dE/dt}$$

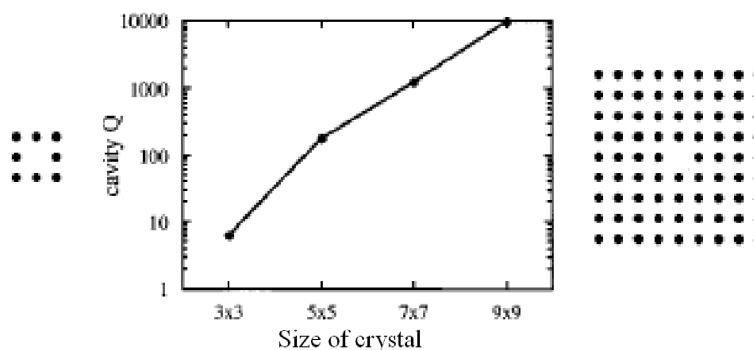


Fig. 4: Quality factor as a function of the size of the crystal.

where E is the stored energy, T_0 is the resonant frequency and $P = -\frac{dE}{dt}$ is the dissipated power. A resonator can

there fore substation Q oscillations before its energy decays by a factor of e^{-Q} of its original value. After exciting the resonant mode, the total energy can be monitored as a function of time and Q can be computed from the number of optical cycles required for the energy to decay. Before presenting the results, we note that the Q factor could also have been computed using a different method. We recall that Q can be defined as $\frac{\omega_0}{\Delta\omega}$, where

$\Delta\omega$ is the full width at half-power of the resonators Lorentzian response. By computing $\Delta\omega$ from transmission calculation, we could have estimated the value of Q . This method, however, would have led to larger uncertainties, especially for large values of Q . we consider again a finite-sized crystal made of dielectric rods where a single rod has been removed. The crystal dimensions $N \times N$, where N is an odd number. We compute Q for several values of N .

The value of Q is shown in fig. 4 as a function of the size of the crystal. Q increases exponentially with the number of rods. It reaches a value close to 10^4 with as little as four lattices on either side of the defect, in agreement with our previous results, which showed strong confinement at the resonance. Since the only energy loss in the structure occurs by tunneling through the edges of the crystal, Q does not saturate even for a very large number of rods.

CONCLUSION

By introducing a defect in a photonic crystal, sharp resonant states can be created in the vicinity of the defect. The properties of these modes frequency, polarization and field distribution can be controlled by changing the nature and the size of the defect.

Furthermore the quality factor Q increases exponentially with the crystals size.

REFERENCES

1. Taflove Allen and C. Hagness Susan, 2000. Computational Electrodynamics: The Finite-Difference Time-Domain Method, 2nd ed., 2000, Artech House Publishers, ISBN 1-58053-076-1.
2. Steven G. Johnson and J.D. Joannopoulos, 2003. Introduction to Photonic Crystal, Bloch's Theorem Band Diagram and Gaps (But No Defects), MIT 3rd February 2003.
3. Min, B.K., J.E. Kim and H.Y. Park, 2004. Channel drop filters using resonant tunneling processes in two dimensional triangular lattice photonic crystal slabs, Opt. Commun., 237: 59-63.
4. Integrated Photonics Laboratory School of Electrical Engineering Sharif University of Technology, 2005. PWE and Methods for Analysis of photonic Crystals.
5. Shinya, S.A., M. Notomi Mitsugi, E. Kuramochi, T. Kawabata, S. Kondo, T. Watanabe and T. Tsuchizawa, 2004. Photonic crystal devices combining width tuned waveguides and cavities, in Technical Digest of International Symposium on Photonic and Electronic Crystal Structures V, (Kyoto, Japan, 2004).
6. Kee, C.S., D.H. Cho, J.H. Jung, I. Park, H. Lim, S.G. Lee and H. Han, 2003. Photonic crystal multi-channel add/drop filters, in Abstract book of MRS 2003 Spring meeting, (San Francisco, Calif., 2003), pp: 64.
7. Dorazio, A., M. De Sario, V. Marrocco and F. Prudenzano, 2008. Photonic crystal drop Filter Exploiting Resonant Cavity Configuration, IEEE Transaction on Nanotechnology, 7(1).

8. Bahrami, M., M.S. Abrishamian and S.A. Mirtaheeri, 2011. Tunable anisotropic photonic crystal channel-drop filter, *Journal of Optics*, 13(1).
9. Yablonovitch, E., T.J. Gmitter and K.M. Leung, 1991. *Phys. Rev. Lett.*, 67(17): 2295.
10. Pierr R. Villeneuve, Shanhui Fan and J.D. Joannopoulos, 1996. Microcavities in photonic crystals mode symmetry, tunability and coupling efficiency, *The American Physical Society*, 54(11): 15.
11. *Integrated Photnics Laberatory School of Electrical Engineering sharif University of Technology*, 2005. *PWE and Methods for Analysis of photonic Crystals*.